JCI The Journal of Clinical Investigation

Kras^{G12D} and *Nkx2-1* haploinsufficiency induce mucinous adenocarcinoma of the lung

Yutaka Maeda, … , Takeshi Nagayasu, Jeffrey A. Whitsett

J Clin Invest. 2012;122(12):4388-4400. https://doi.org/10.1172/JCI64048.

Research Article **Oncology**

Mucinous adenocarcinoma of the lung is a subtype of highly invasive pulmonary tumors and is associated with decreased or absent expression of the transcription factor NK2 homeobox 1 (NKX2-1; also known as TTF-1). Here, we show that haploinsufficiency of *Nkx2-1* in combination with oncogenic *Kras*^{G12D}, but not with oncogenic *EGFR*^{L858R}, caused pulmonary tumors in transgenic mice that were phenotypically similar to human mucinous adenocarcinomas. Gene expression patterns distinguished tumor goblet (mucous) cells from nontumorigenic airway and intestinal goblet cells. Expression of NKX2-1 inhibited urethane and oncogenic *Kras*^{G12D}-induced tumorigenesis in vivo. Haploinsufficiency of *Nkx2-1* enhanced *Kras*^{G12D}-mediated tumor progression, but reduced *EGFR*^{L858R}-mediated progression. Genome-wide analysis of gene expression demonstrated that a set of genes induced in mucinous tumors was shared with genes induced in a nontumorigenic chronic lung disease, while a distinct subset of genes was specific to mucinous tumors. ChIP with massively parallel DNA sequencing identified a direct association of NKX2-1 with the genes induced in mucinous tumors. NKX2-1 associated with the AP-1 binding element as well as the canonical NKX2-1 binding element. NKX2-1 inhibited both AP-1 activity and tumor colony formation in vitro. These data demonstrate that NKX2-1 functions in a context-dependent manner in lung tumorigenesis and inhibits *Kras*^{G12D}-driven mucinous pulmonary adenocarcinoma.

Kras^{G12D} and *Nkx2-1* haploinsufficiency induce mucinous adenocarcinoma of the lung

Yutaka Maeda,[1] Tomoshi Tsuchiya,[2] Haiping Hao,[3] David H. Tompkins,[1] Yan Xu,[1] Michael L. Mucenski,[1] Lingling Du,[1] Angela R. Keiser,[1] Takuya Fukazawa,[4] Yoshio Naomoto,[4] Takeshi Nagayasu,[2] and Jeffrey A. Whitsett[1]

[1]Perinatal Institute, Section of Neonatology, Perinatal and Pulmonary Biology, Cincinnati Children's Hospital Medical Center and University of Cincinnati College of Medicine, Cincinnati, Ohio, USA. [2]Division of Surgical Oncology, Department of Translational Medical Sciences, Nagasaki Graduate School of Biomedical Sciences, Nagasaki, Japan. [3]Deep Sequencing and Microarray Core, Johns Hopkins University, Baltimore, Maryland, USA. [4]Department of General Surgery, Kawasaki Medical School, Okayama, Japan.

Mucinous adenocarcinoma of the lung is a subtype of highly invasive pulmonary tumors and is associated with decreased or absent expression of the transcription factor NK2 homeobox 1 (NKX2-1; also known as TTF-1). Here, we show that haploinsufficiency of *Nkx2-1* in combination with oncogenic *Kras*^{G12D}, but not with oncogenic *EGFR*^{L858R}, caused pulmonary tumors in transgenic mice that were phenotypically similar to human mucinous adenocarcinomas. Gene expression patterns distinguished tumor goblet (mucous) cells from nontumorigenic airway and intestinal goblet cells. Expression of NKX2-1 inhibited urethane and oncogenic *Kras*^{G12D}-induced tumorigenesis in vivo. Haploinsufficiency of *Nkx2-1* enhanced *Kras*^{G12D}-mediated tumor progression, but reduced *EGFR*^{L858R}-mediated progression. Genome-wide analysis of gene expression demonstrated that a set of genes induced in mucinous tumors was shared with genes induced in a nontumorigenic chronic lung disease, while a distinct subset of genes was specific to mucinous tumors. ChIP with massively parallel DNA sequencing identified a direct association of NKX2-1 with the genes induced in mucinous tumors. NKX2-1 associated with the AP-1 binding element as well as the canonical NKX2-1 binding element. NKX2-1 inhibited both AP-1 activity and tumor colony formation in vitro. These data demonstrate that NKX2-1 functions in a context-dependent manner in lung tumorigenesis and inhibits *Kras*^{G12D}-driven mucinous pulmonary adenocarcinoma.

Introduction

Mucinous adenocarcinoma of the lung (formerly known as mucinous bronchioalveolar cancer) is pathologically classified as tumor cells with goblet cell morphology containing abundant intracytoplasmic mucin (1). Invasive mucinous adenocarcinoma of the lung has a higher malignant potential than do the more common types of lung adenocarcinoma, such as acinar or papillary adenocarcinoma. Mucinous adenocarcinoma of the lung is associated with decreased or absent expression of the transcription factor NK2 homeobox 1 (NKX2-1; also known as TTF-1) and the expression of mucins, including mucin 5AC, oligomeric mucus/gel-forming (MUC5AC). Genetically, approximately 76% of mucinous adenocarcinomas of the lung have *KRAS* mutations, a frequent mutation in lung adenocarcinoma associated with tobacco use (2), but mucinous adenocarcinoma of the lung is rarely associated with *EGFR* mutations. In contrast, nonmucinous lung adenocarcinoma is frequently associated with *EGFR* mutations (~45%), but less frequently with *KRAS* mutations (~13%; ref. 1).

NKX2-1 plays a critical role in lung morphogenesis and respiratory epithelial-specific gene expression, including activation of surfactant proteins and repression of mucins (3, 4). The potential oncogenic role of NKX2-1 in the pathogenesis of adenocarcinoma of the lung was proposed by findings that a region of 14q13.3 containing *NKX2-1*, *NKX2-8*, and *PAX9* was amplified in approximately 10% of human lung adenocarcinoma (5–7). Loss-of-function and gain-of-function studies in human lung carcinoma and transformed cells supported a role of *NKX2-1* as an oncogene (5–9); however, the *Kras*$^{LSL–G12D/+}$;*p53*$^{-/-}$ mouse model and a xenograft mouse model supported the concept that NKX2-1 is an antimetastatic factor (10, 11).

Here, we present what we believe to be a novel mouse model that develops mucinous adenocarcinoma of the lung, in which oncogenic *Kras*^{G12D} is induced in the respiratory epithelium of *Nkx2-1* heterozygous (*Nkx2-1*$^{+/-}$) mice. Reduced expression of *Nkx2-1* promoted initiation and progression of invasive *Kras*^{G12D}-induced mucinous lung adenocarcinoma. Conversely, increased expression of NKX2-1 in the respiratory epithelium inhibited carcinogen- or *Kras*^{G12D}-induced lung tumor formation in vivo. A genome-wide gene expression study indicated that NKX2-1 inhibited mRNAs involved in tumorigenesis and induced genes involved in apoptosis. Expression of NKX2-1 sensitized lung carcinoma cells to cisplatin-induced apoptosis in vitro. ChIP sequencing (ChIP-seq) analysis indicated that NKX2-1 directly associated with a set of genes induced in mucinous tumors. Bioinformatic analysis identified the AP-1 binding element (TGAnTCA) in a portion of the NKX2-1 ChIP-seq peaks. NKX2-1 inhibited AP-1–mediated activity and tumor colony formation in vitro, which suggested that NKX2-1 suppresses lung tumorigenesis, at least in part, by inhibiting AP-1 activity. Our findings provide a molecular mechanism by which NKX2-1 suppresses mutant *Kras*–driven mucinous adenocarcinoma.

Results

Haploinsufficiency of Nkx2-1 induced mucinous adenocarcinomas during Kras^{G12D} *tumorigenesis.* In order to determine whether reduced expression of *Nkx2-1* influences the pathogenesis of invasive mucinous adenocarcinoma of the lung, we created a mouse model

Conflict of interest: The authors have declared that no conflict of interest exists.

Citation for this article: *J Clin Invest.* 2012;122(12):4388–4400. doi:10.1172/JCI64048.

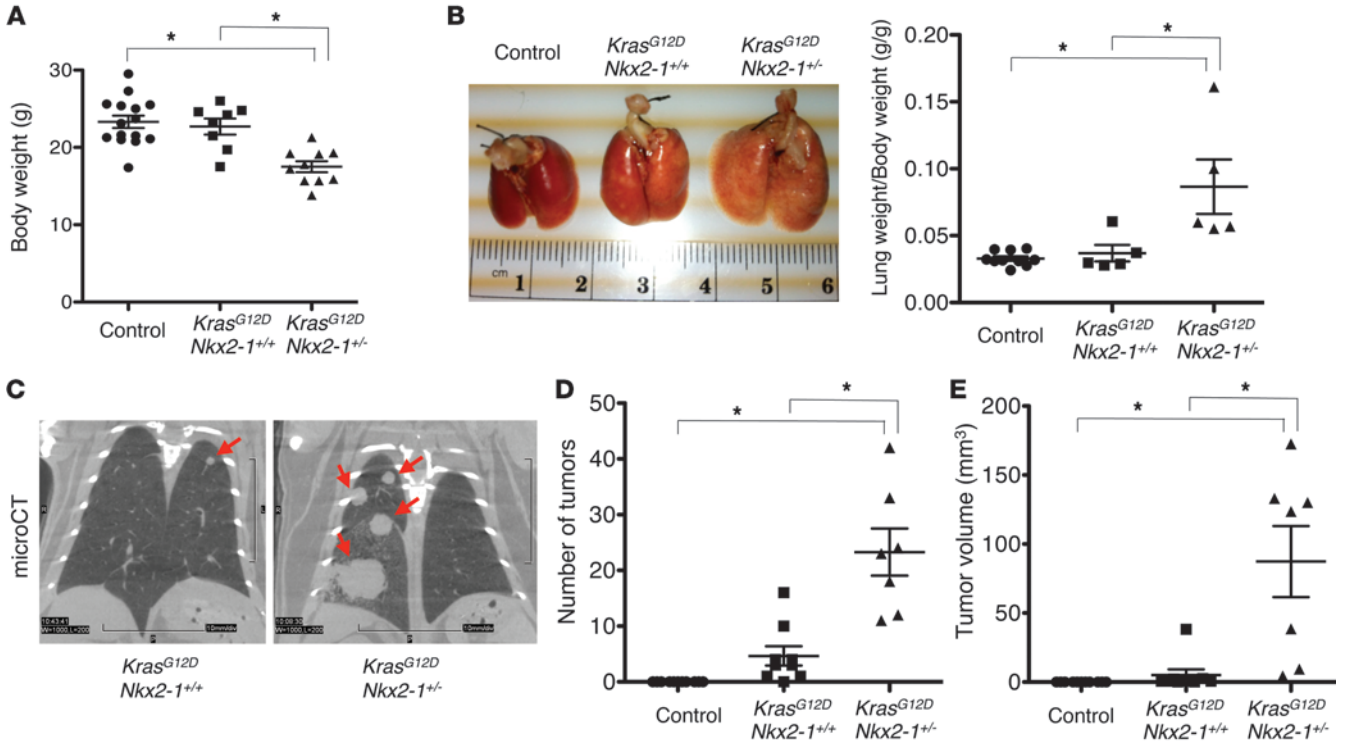

Figure 1
Haploinsufficiency of *Nkx2-1* increased tumorigenesis in *Kras*^{G12D} mice. (**A**) *Kras*^{G12D};*Nkx2-1*$^{+/-}$ mice (n = 10) lost weight compared with *Kras*^{G12D};*Nkx2-1*$^{+/+}$ (n = 8) and control (n = 15) mice 2 months after Dox administration. (**B**) *Kras*^{G12D};*Nkx2-1*$^{+/-}$ mice (n = 5) had larger lungs than did *Kras*^{G12D};*Nkx2-1*$^{+/+}$ (n = 5) and control (n = 10) mice 2 months after Dox administration. (**C**) *Kras*^{G12D};*Nkx2-1*$^{+/-}$ mice developed lung tumors (arrows), detected by microCT, 8 months after Dox administration. (**D** and **E**) Number (**D**) and volume (**E**) of lung tumors measured by microCT increased in *Kras*^{G12D};*Nkx2-1*$^{+/-}$ (n = 7) compared with *Kras*^{G12D};*Nkx2-1*$^{+/+}$ (n = 9) and control (n = 11) mice 8 months after Dox administration. All results are mean ± SEM. *P < 0.05.

in which mutated active *Kras* was conditionally expressed in the respiratory epithelium of wild-type or heterozygous *Nkx2-1* mice. Mice were developed by crossing transgenic *Scgb1a1-rtTA;[tetO]-Kras4b*^{G12D} mice (12) with *Nkx2-1*$^{+/-}$ mice (13). *Nkx2-1* mRNA was significantly reduced in *Nkx2-1*$^{+/-}$ versus *Nkx2-1*$^{+/+}$ mice (4, 14). At 2 months after doxycycline (Dox) administration, the *Kras* transgenic mice with heterozygous *Nkx2-1* (*Scgb1a1-rtTA;[tetO]-Kras4b*^{G12D};*Nkx2-1*$^{+/-}$; referred to herein as *Kras*^{G12D};*Nkx2-1*$^{+/-}$) lost weight compared with the *Kras* transgenic mice with wild-type *Nkx2-1* (*Scgb1a1-rtTA;[tetO]-Kras4b*^{G12D};*Nkx2-1*$^{+/+}$; referred to herein as *Kras*^{G12D};*Nkx2-1*$^{+/+}$) and control littermates (Figure 1A). Average lung volume in *Kras*^{G12D};*Nkx2-1*$^{+/-}$ mice was increased compared with *Kras*^{G12D};*Nkx2-1*$^{+/+}$ and control mice (Figure 1B). Tumor number and volume of *Kras*^{G12D};*Nkx2-1*$^{+/-}$ mice, as detected by microCT (Figure 1C), increased compared with those of *Kras*^{G12D};*Nkx2-1*$^{+/+}$ and control mice (Figure 1, D and E). In the absence of *Kras*^{G12D}, weights of *Nkx2-1*$^{+/-}$ and *Nkx2-1*$^{+/+}$ mice were similar (Supplemental Figure 1; supplemental material available online with this article; doi:10.1172/JCI64048DS1). *Nkx2-1*$^{+/-}$ mice did not develop spontaneous lung tumors at 9 months of age (data not shown). Whereas *Kras*^{G12D};*Nkx2-1*$^{+/+}$ mice developed benign lung adenoma, *Kras*^{G12D};*Nkx2-1*$^{+/-}$ mice developed invasive lung adenocarcinoma within 2–8 months (Figure 2). Unlike tumor cells in *Kras*^{G12D};*Nkx2-1*$^{+/+}$ mice, tumor cells in *Kras*^{G12D};*Nkx2-1*$^{+/-}$ mice contained abundant intracytoplasmic mucin and lacked NKX2-1 staining (Figure 2A), consistent with the histochemical features of human mucinous adenocarcinoma of the lung (Supplemental Figure 2). Human mucinous adenocarcinomas often consist of a heterogeneous mixture of tumor cell types, including features of papillary or acinar adenocarcinoma (1). In the *Kras*^{G12D};*Nkx2-1*$^{+/-}$ mouse model, the percentage of tumor goblet cells (stained with the intracytoplasmic goblet cell marker anterior gradient homolog 2 [AGR2]) was 35% (Supplemental Figure 3). Cytokeratin 7 (CK7) and cytokeratin 20 (CK20), clinical biomarkers for mucinous adenocarcinoma of the lung (1), were expressed in *Kras*^{G12D};*Nkx2-1*$^{+/-}$ mice, whereas only CK7 was present in *Kras*^{G12D};*Nkx2-1*$^{+/+}$ mice (Figure 2B). When Dox was administered for 2 months and then withdrawn for 2 weeks, tumors regressed (Figure 2C), which indicates that ongoing expression of mutant *Kras* is required for the maintenance of tumor goblet cells.

Tumor goblet cells were not dependent on the SPDEF/FOXA3 transcriptional program. Mucous metaplasia is a prominent feature of various chronic lung diseases, including asthma, chronic obstructive pulmonary disease (COPD), and cystic fibrosis (CF). Mucous metaplasia in these non-neoplastic disorders is associated with increased expression of the transcription factors Sam pointed domain Ets-like factor (SPDEF) and FOXA3, as well as various mucins, including MUC5AC, and mucin-associated genes, including AGR2 (15). To assess whether goblet cells associated with *Kras*^{G12D};*Nkx2-1*$^{+/-}$–induced tumors shared features with nontumor goblet cells, we

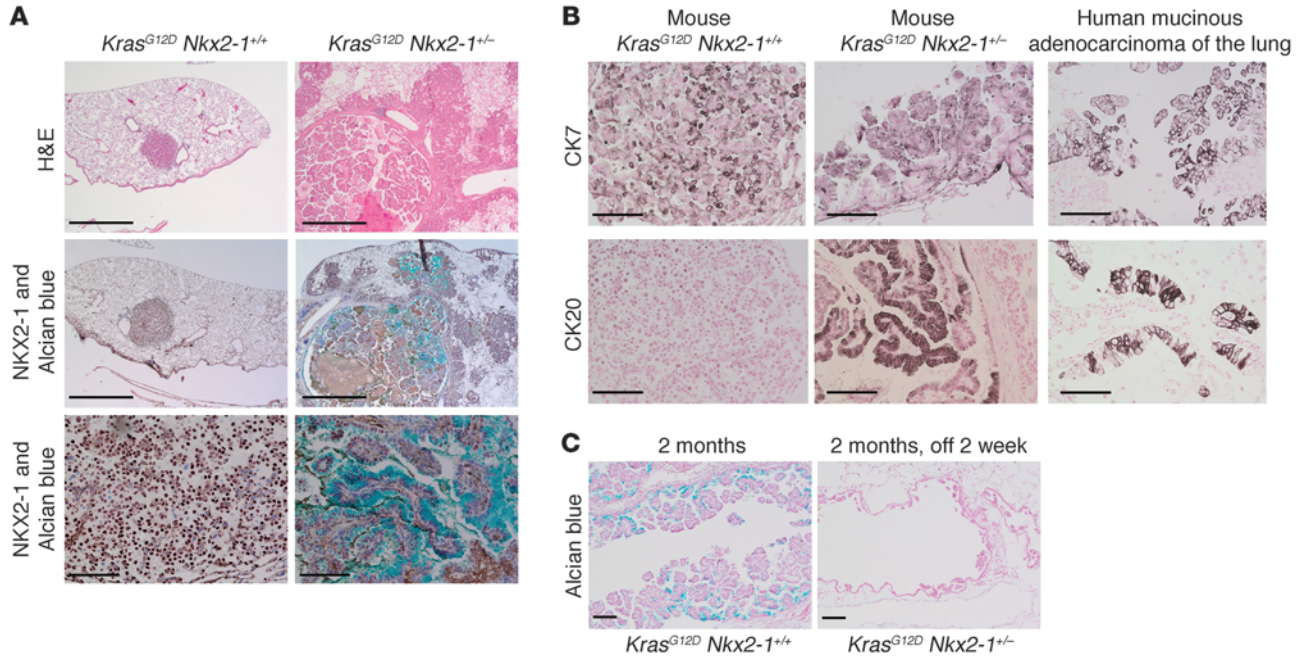

Figure 2

Haploinsufficiency of *Nkx2-1* caused mucinous adenocarcinoma of the lung in *Kras*^{G12D} mice. (**A**) Lung sections were stained with H&E or with NKX2-1 and Alcian blue. Tumors in *Kras*^{G12D}*;Nkx2-1*$^{+/–}$ mice (14 of 16) contained goblet cells with abundant intracytoplasmic mucin (Alcian blue positive, NKX2-1 negative). (**B**) CK7 and CK20, clinical biomarkers for human mucinous adenocarcinoma of the lung, were expressed in tumor cells of *Kras*^{G12D}*;Nkx2-1*$^{+/–}$ mice. (**C**) Alcian blue–stained tumor cells in lungs of *Kras*^{G12D}*;Nkx2-1*$^{+/–}$ mice 2 months after Dox administration (left; $n = 6$). Tumor cells in *Kras*^{G12D}*;Nkx2-1*$^{+/–}$ mice regressed following withdrawal of Dox for 2 weeks after the 2-month administration (right; $n = 8$). Scale bars: 1 mm (**A**, top and middle); 100 μm (**A**, bottom, and **B** and **C**).

compared immunohistochemical findings of the mutant *Kras*–induced mucinous tumors with mucous metaplasia induced by house dust mite (HDM) allergen exposure (Figure 3). Mucus-associated proteins, including MUC5AC, MUC5B, and AGR2, were readily detected in goblet cells in lung tumors of *Kras*^{G12D}*;Nkx2-1*$^{+/–}$ mice and in airways of HDM-challenged mice, but were absent in tumors induced in *Kras*^{G12D}*;Nkx2-1*$^{+/+}$ mice. In allergen-induced mouse models, NKX2-1 and FOXA2 inhibit goblet cell differentiation, whereas SPDEF is required for airway mucous metaplasia (4, 15, 16). Consistent with their inhibitory roles in goblet cell differentiation, both NKX2-1 and FOXA2 were decreased in tumor goblet cells in *Kras*^{G12D}*;Nkx2-1*$^{+/–}$ mice (Figure 2A and Figure 3). Both SPDEF and FOXA3 were highly expressed in airway goblet cells after HDM exposure, as previously reported (15, 17), but were not detected in the goblet cells in *Kras*^{G12D}*;Nkx2-1*$^{+/–}$–induced tumors (Figure 3 and Supplemental Figure 4).

NKX2-1 inhibited mutant Kras–induced tumorigenesis in vivo. To directly assess the role of NKX2-1 in lung tumorigenesis, NKX2-1 was conditionally expressed in respiratory epithelial cells (4). This conditional system has been widely used to model lung tumorigenesis in mice (12, 18, 19). To assess whether increased NKX2-1 is sufficient to initiate tumor formation, Dox was administered to *Scgb1a1-rtTA;[tetO]–Flag–Nkx2-1* mice for approximately 6–12 months, after which time none of the NKX2-1–expressing mice developed lung tumors ($n = 19$; data not shown). Kendall et al. reported that *NKX2-1*, *NKX2-8*, and *PAX9* resided within the 14q13.3 locus and were amplified in approximately 10% of lung adenocarcinomas; in vitro data demonstrated that the combination of NKX2-1 with either NKX2-8 or PAX9 was required for colony formation in virus-transformed human bronchial epithelial cells in vitro (5). We generated transgenic mice coexpressing NKX2-1 and NKX2-8 or NKX2-1 and PAX9. Coexpression of NKX2-1 with either PAX9 or NKX2-8 did not cause tumorigenesis after 4 months of Dox administration (Supplemental Figure 5).

To assess whether NKX2-1 influences tumorigenesis in *Scgb1a1-rtTA;[tetO]–Flag–Nkx2-1* transgenic mice (both transgenic mice; FVB/N background), we treated the mice with urethane, a lung carcinogen. Urethane-induced tumors were readily detected on the lung surface of FVB/N control mice 16 weeks after administration (20). Expression of NKX2-1 decreased the number of urethane-induced tumors (Table 1 and Figure 4, A and B), which indicates that increased NKX2-1 suppresses tumor initiation. The few tumors seen in the NKX2-1–induced transgenic mouse group (*Scgb1a1-rtTA;[tetO]–Flag–Nkx2-1* on Dox) did not express FLAG–NKX2-1 (data not shown), and they may be derived from lung epithelial cells that did not express the *Scgb1a1-rtTA* transgene. Since urethane induces lung tumors associated with *Kras* mutations (21), we assessed whether NKX2-1 inhibited mutant *Kras*–induced tumors by creating *Nkx2-1;Kras*^{G12D} triple transgenic mice (*Scgb1a1-rtTA;[tetO]–Flag–Nkx2-1;[tetO]-Kras4b*^{G12D}). Coexpression of NKX2-1 reduced the number and volume of *Kras*^{G12D}-induced lung tumors (Figure 4, C and D), which indicates that increased expression of NKX2-1 inhibited mutant *Kras*–induced tumor initiation and progression in vivo.

We also assessed whether NKX2-1 influences proliferation of lung epithelial cells by using HBEC3 human bronchial epithelial cells generated by expression of hTERT and CDK4 (22). We infected HBEC3

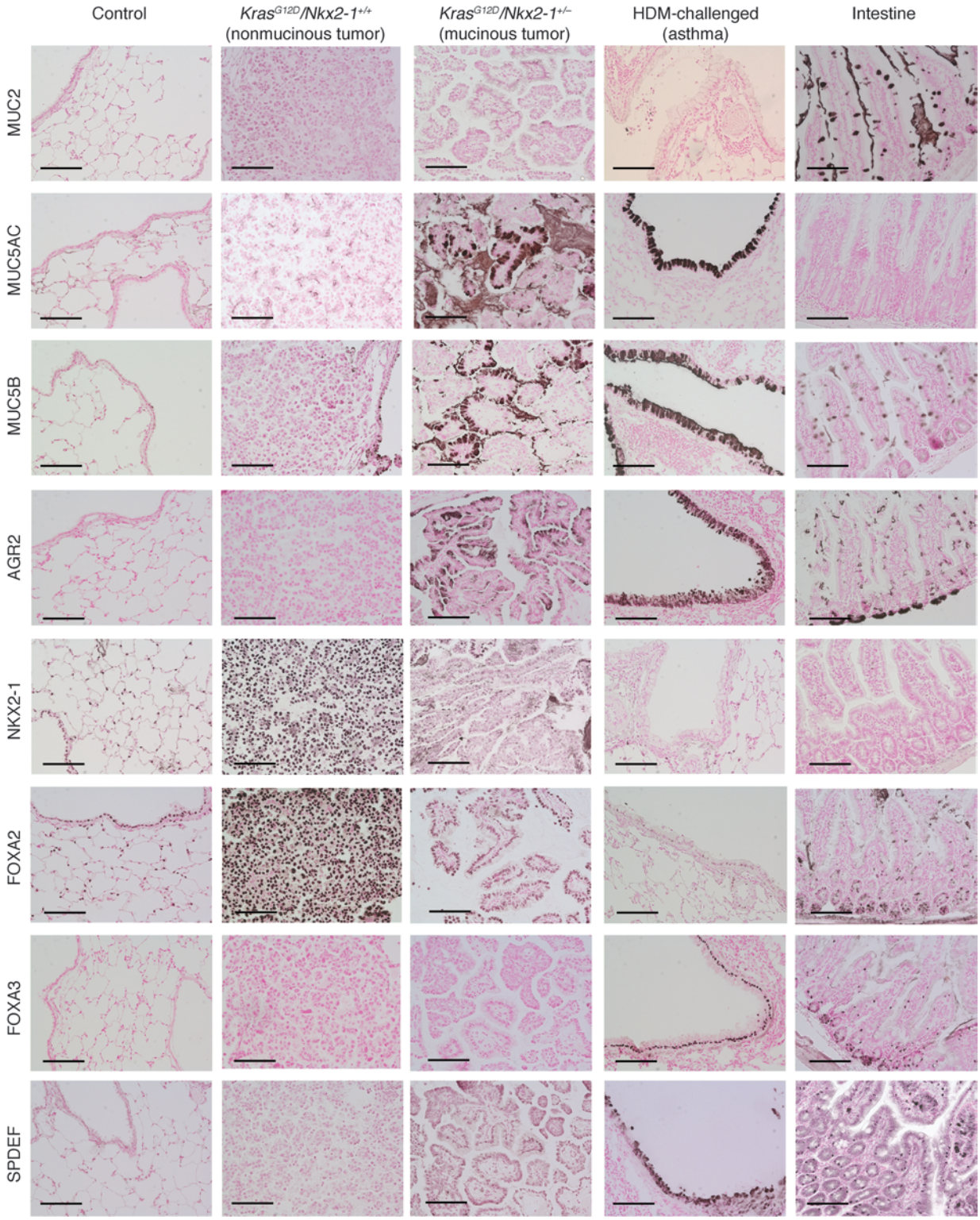

Figure 3
Tumor goblet cells are not dependent on the SPDEF/FOXA3 transcriptional program. Sections from control, *Kras*^{G12D}*;Nkx2-1*$^{+/+}$, *Kras*^{G12D}*;Nkx2-1*$^{+/-}$, and HDM-challenged lungs and normal intestine were stained for mucins MUC2, MUC5AC, MUC5B, and AGR2 and the transcription factors NKX2-1, FOXA2, FOXA3, and SPDEF. FOXA3 and SPDEF, which were seen in goblet cells of HDM-challenged lungs, were not expressed in the tumor goblet cells of *Kras*^{G12D}*;Nkx2-1*$^{+/-}$ mice. Scale bars: 100 μm.

Table 1
Lung tumor development after exposure to urethane

Mouse group	Transgenic mouse	Dox	Tumor incidence[A]
Control	*Scgb1a1-rtTA*	Yes	15/15
Control	*[tetO]–Flag–Nkx2-1*	Yes	8/8
Control	*Scgb1a1-rtTA;[tetO]–Flag–Nkx2-1*	No	15/15
NKX2-1 induced	*Scgb1a1-rtTA;[tetO]–Flag–Nkx2-1*	Yes	6/16

[A]Number of mice that developed lung tumors relative to total.

cells with a lentiviral vector containing *Flag–Nkx2-1* (4). Expression of NKX2-1 significantly inhibited proliferation of HBEC3 cells (Supplemental Figure 6), which suggests that NKX2-1 may influence tumorigenesis, at least in part, by suppressing cell proliferation.

Haploinsufficiency of Nkx2-1 did not induce mucinous adenocarcinomas during EGFR^{L858R} tumorigenesis. *EGFR* mutations are not associated with human mucinous adenocarcinoma (1). While mutant *Kras*–induced lung tumorigenesis was suppressed by NKX2-1 in vivo (present study and ref. 10), whether mutant *EGFR*–induced lung tumorigenesis is influenced by NKX2-1 in vivo is unknown. Mutated active *EGFR^{L858R}* was conditionally expressed in the respiratory epithelium of wild-type or *Nkx2-1$^{+/-}$* mice by crossing *Scgb1a1-rtTA;[tetO]-EGFR^{L858R}* mice (18) with the *Nkx2-1$^{+/-}$* mice (13); these mice are referred to herein as *EGFR^{L858R};Nkx2-1$^{+/+}$* and *EGFR^{L858R};Nkx2-1$^{+/-}$*, respectively. Unexpectedly, tumor number and volume were significantly decreased in *EGFR^{L858R};Nkx2-1$^{+/-}$* mice compared with *EGFR^{L858R};Nkx2-1$^{+/+}$* littermates (Figure 5A), which indicates that tumorigenesis mediated by mutant *EGFR* was enhanced by NKX2-1. Consistent with the infrequent presence of *EGFR* mutations in human mucinous adenocarcinoma of the lung (1), neither *EGFR^{L858R};Nkx2-1$^{+/+}$* nor *EGFR^{L858R};Nkx2-1$^{+/-}$* mice developed mucinous adenocarcinomas (Figure 5B). Lung tumors in *EGFR^{L858R};Nkx2-1$^{+/-}$* mice stained for MUC5B, but not Alcian blue or MUC5AC. These results indicate that (a) NKX2-1 enhances tumorigenesis in the context of an activated mutant *EGFR*, and (b) the mutant *EGFR* did not induce tumor goblet cells in *Nkx2-1$^{+/-}$* mice. Consistent with these mouse data, the majority of the *KRAS* mutation–associated human adenocarcinoma cell lines expressed high levels of *MUC5AC* mRNA, whereas all cell lines bearing *EGFR* mutations expressed little or no *MUC5AC* mRNA (Figure 5C). Of *KRAS* mutant cell lines, those lacking *NKX2-1* expressed higher levels of *MUC5AC* and *MUC5B* mRNA than did those positive for *NKX2-1* (Figure 5C), which suggests that NKX2-1 suppresses mucin gene expression in mutant *KRAS*–associated tumors.

NKX2-1 inhibited expression of a group of genes induced in mucinous tumors. To identify mechanisms underlying the pathogenesis of mucinous adenocarcinoma of the lung, genome-wide gene expression analysis was performed using *Kras^{G12D};Nkx2-1$^{+/-}$* mouse lungs. A number of mRNAs that were increased in *Kras^{G12D};Nkx2-1$^{+/-}$* lungs overlapped with those induced in a HDM model of asthma (HDM-challenged mice; ref. 23), including *ADAM8*, *AGR2*, *ALOX15*, *CHI3L4*, *IGF1*, *MUC5AC*, *MUC5B*, *RETNLA*, and *SAA3* (Figure 6, highlighted in blue and green, and Supplemental Table 2), which supports the concept that some of the aspects of goblet cell differentiation are shared among these lung diseases. In order to identify genes regulated by NKX2-1 in the mucinous tumor model, mRNA analysis was performed in A549 human lung carcinoma cells, which bear a *KRAS* mutation and lack *NKX2-1* expression (Figure 5C). NKX2-1 was expressed in the A549 cells with a lentiviral vector (Supplemental Table 3 and ref. 4). A group of NKX2-1–inhibited genes induced in the lungs of the mucinous tumor model, but not in the asthma model, was identified (Figure 6, highlighted in red). Those genes may be tumor markers or function as tumor promoters. *AGR2*, *LCN2*, *MUC5AC*, *MUC5B*, and *RBP4* were also NKX2-1–inhibited genes; however, they were expressed in lungs of both the mucinous tumor and the HDM-induced mouse models (Figure 6, highlighted in green).

NKX2-1 inhibited expression of genes related to lung tumorigenesis and induced those involved in cell death. The expression profile of genes regulated by NKX2-1 in A549 human lung carcinoma cells is shown in Figure 6, Figure 7A, and Supplemental Table 3. NKX2-1 induced expression of *SFTPA*, *SFTPB*, *LAMP3*, *CEACAM6*, and *MYBPH* (3, 11, 24). Expression of *MUC5AC*, *MUC5B*, and *SERPINE1* (4, 25) was inhibited by NKX2-1. Gene Ontology analysis revealed that expression of genes linked to *protein kinase cascade* and *enzyme linked receptor protein signaling pathway* was decreased, and expression of those related to *programmed cell death* was increased, by NKX2-1 (Supplemental Figure 7). NKX2-1 inhibited *FGFR1*, *FGFR4*, *IGF1R*, *CCND3*, *CCNE2*, and *CDK6*, which are associated with cancer (26–31), but induced expression of genes that induce programmed cell death, such as *FAS* and *TIMP3* (32, 33). Although NKX2-1 suppressed genes linked to tumorigenesis and induced genes linked to apoptosis, it did not alter viability of A549 carcinoma cells (data not shown). Since expression of NKX2-1 in human lung tumors is associated with better prognosis (34), we assessed whether NKX2-1 influenced chemotherapy-induced cell death in A549 cells. Cisplatin is a chemotherapy drug clinically used to treat mutant *KRAS*–associated lung cancer (35). NKX2-1 sensitized A549 cells to cisplatin-induced apoptosis, a finding confirmed by detection of cleaved PARP, an apoptosis marker (Figure 7, B–D).

ChIP-seq analysis identified NKX2-1 binding sites in A549 lung carcinoma cells. ChIP-seq analysis was used to identify potential direct transcriptional targets of NKX2-1 in chromatin from A549 cells expressing NKX2-1. Sequence reads obtained from massively parallel sequencing were mapped onto the human genome. ChIP-seq analysis was validated by examining NKX2-1 binding peaks in the promoter of *SFTPA1*, a known downstream target of NKX2-1 (36, 37). NKX2-1 was directly associated with the promoter of the *SFTPA1* gene (Figure 8A). NKX2-1 inhibited expression of *MUC5AC* (Figure 6 and Figure 7A) and was directly associated with the promoter of *MUC5AC* (Figure 8B), suggestive of its activity as a transcriptional suppressor. NKX2-1 was also associated with the first and second introns of *FGFR1* (Figure 8C), a known oncogene (26), and inhibited *FGFR1* mRNA in A549 cells (Figure 7A).

NKX2-1 binding elements were present in intergenic, intronic, 5′ untranslated (5′UTR), and upstream regions (Supplemental Figure 8). The widespread distribution of NKX2-1 binding sites observed in the present study is consistent with other ChIP-seq analyses identifying STAT1, GATA1, and MYOD binding elements in the genome. The potential regulatory role of the widespread binding of transcription factors in chromatin looping, chromatin organization, and nuclear structure has been proposed; however, their precise biological roles remain unknown (38). To assess the functional significance of direct associations of NKX2-1 with chromatin, we analyzed ChIP-seq locations that occurred within 10 kb of those genes that were up- or down-regulated by NKX2-1 (Figure 6, Figure 7A, and Supplemental

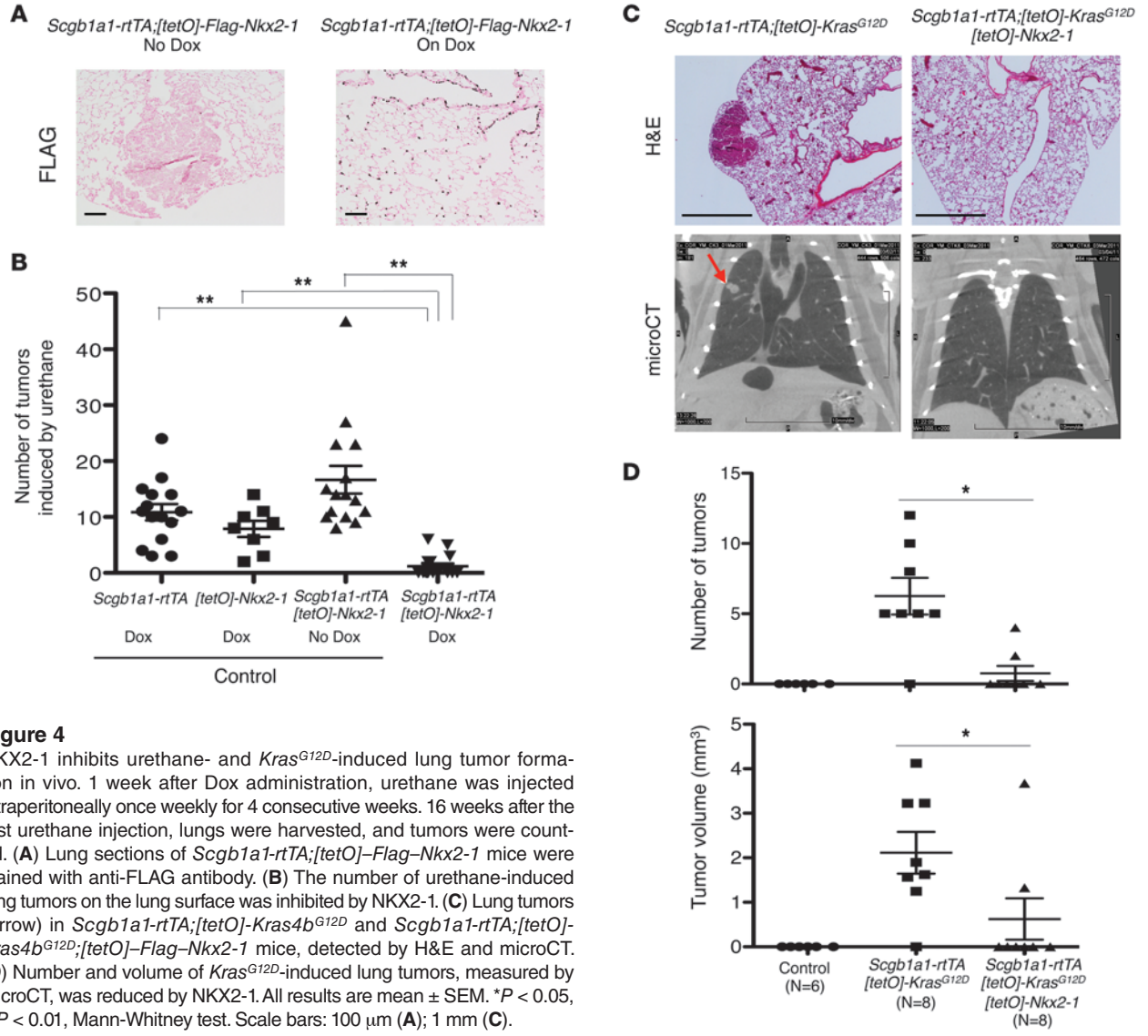

Figure 4

NKX2-1 inhibits urethane- and *Kras*^{G12D}-induced lung tumor formation in vivo. 1 week after Dox administration, urethane was injected intraperitoneally once weekly for 4 consecutive weeks. 16 weeks after the first urethane injection, lungs were harvested, and tumors were counted. (**A**) Lung sections of *Scgb1a1-rtTA;[tetO]–Flag–Nkx2-1* mice were stained with anti-FLAG antibody. (**B**) The number of urethane-induced lung tumors on the lung surface was inhibited by NKX2-1. (**C**) Lung tumors (arrow) in *Scgb1a1-rtTA;[tetO]-Kras4b*^{G12D} and *Scgb1a1-rtTA;[tetO]-Kras4b*^{G12D}*;[tetO]–Flag–Nkx2-1* mice, detected by H&E and microCT. (**D**) Number and volume of *Kras*^{G12D}-induced lung tumors, measured by microCT, was reduced by NKX2-1. All results are mean ± SEM. **P* < 0.05, ***P* < 0.01, Mann-Whitney test. Scale bars: 100 μm (**A**); 1 mm (**C**).

Table 3). The distribution of the locations within the subregions of each gene was obtained (Figure 8D). The first intron was treated as a separate region, as it is thought to be involved in transcription control in the human genome (39). In NKX2-1–upregulated genes, 46% of NKX2-1 peaks were located upstream of the second exon, including 10 kb upstream, 5′UTR, and the first intron. Approximately 38% of the peaks were located in the other introns. In contrast, in NKX2-1–downregulated genes, 39% of NKX2-1 peaks were located upstream of the second exon, while 43% of the peaks were located in the other introns (Figure 8D), indicative of the presence of potential inhibitory NKX2-1 regulatory sites linked more closely to regions downstream of the second exon. Binding to 3′ proximal regions, including 3′UTR and 10 kb downstream, was similar between upregulated and downregulated genes (14% vs. 15%). NKX2-1 binding sites were not detected in the first exons.

NKX2-1 associated with canonical AP-1 binding sites. Binding sequences that were associated with NKX2-1 were analyzed to identify overrepresented motifs. As expected, NKX2-1 associated with the motif CTTG (reverse complement CAAG), as seen in the promoter of *SFTPA1* (Figure 8, A and E), consistent with previous studies (40). A high-frequency association of NKX2-1 with TGAGTCA (reverse complement TGACTCA), an established binding motif for the transcription factor AP-1 (Figure 8E and Supplemental Figure 9), was identified. Among the NKX2-1–targeted genes induced in the present mucinous tumor model (Figure 6), 43% of them (13 of 30) had the AP-1 motif identified in the NKX2-1–ChIP-seq peaks (Supplemental Figure 10). AP-1 is an oncoprotein strongly associated with lung cancer (41). AP-1 is also known to activate *MUC5AC* through the JNK–AP-1 pathway (42, 43). NKX2-1 was associated with an AP-1 binding site in the *MUC5AC* promoter (Figure 8B). In order to assess the functional relevance of the association of NKX2-1 with the AP-1 binding element, an AP-1 reporter luciferase construct containing AP-1 binding elements was cotransfected with a NKX2-1 expression vector. As shown in Figure 8F, AP-1 activity in H441 human lung adenocarcinoma cells was significantly inhibited by NKX2-1. Other lung epithelial transcription factors, including NKX2-8, CEBPA, FOXA2, or FOXJ1, did not influence AP-1 activity in this assay. The

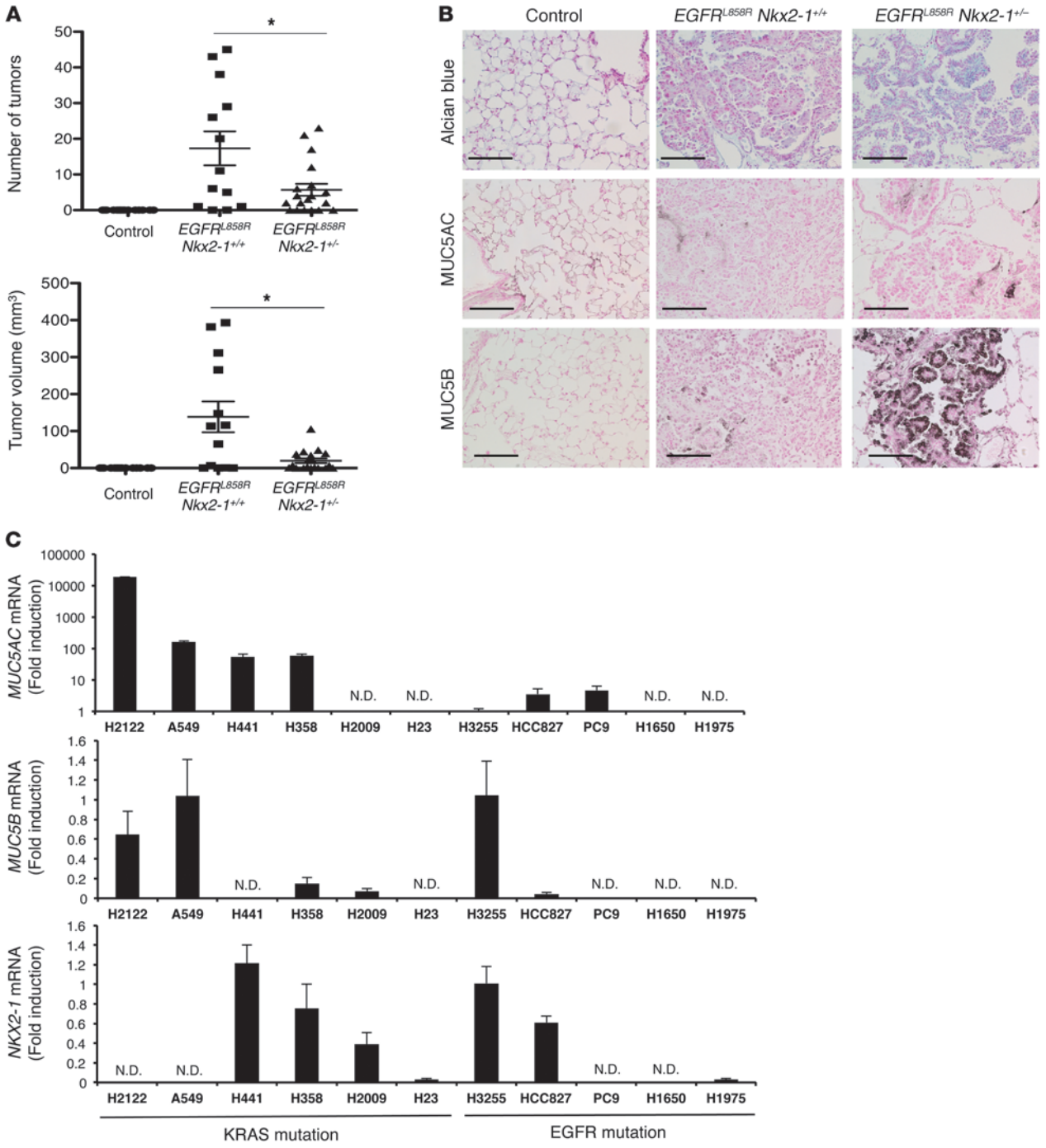

Figure 5

EGFR^{L858R} mice did not develop mucinous adenocarcinoma of the lung regardless of *Nkx2-1* expression. (**A**) Number and volume of lung tumors, measured by microCT, were decreased in *EGFR*^{L858R}*;Nkx2-1*$^{+/-}$ (n = 19) compared with *EGFR*^{L858R}*;Nkx2-1*$^{+/+}$ (n = 13) mice 4 months after Dox administration. n = 16 (control). (**B**) Lung sections were stained with Alcian blue, MUC5AC, and MUC5B. Mucinous tumors were not observed in *EGFR*^{L858R}*;Nkx2-1*$^{+/-}$ or *EGFR*^{L858R}*;Nkx2-1*$^{+/+}$ mice. Tumor cells in lungs of *EGFR*^{L858R}*;Nkx2-1*$^{+/+}$ and *EGFR*^{L858R}*;Nkx2-1*$^{+/-}$ mice did not stain with Alcian blue or MUC5AC, whereas tumor cells in lungs of *EGFR*^{L858R}*;Nkx2-1*$^{+/-}$ mice stained with MUC5B. (**C**) *MUC5AC* mRNA was highly expressed in *NKX2-1*–negative *KRAS* mutant lung carcinoma cell lines (H2122 and A549), but not in *EGFR* mutant lung carcinoma cell lines. *MUC5B* mRNA was expressed in both *KRAS* mutant (H2122 and A549) and *EGFR* mutant (H3255) cell lines. Shown is fold induction compared with mRNA expression of H3255 cells. Results are mean ± SEM (**A**) and mean ± SD of triplicates for each group (**C**). N.D., not detectable. *P < 0.05. Scale bars: 100 μm.

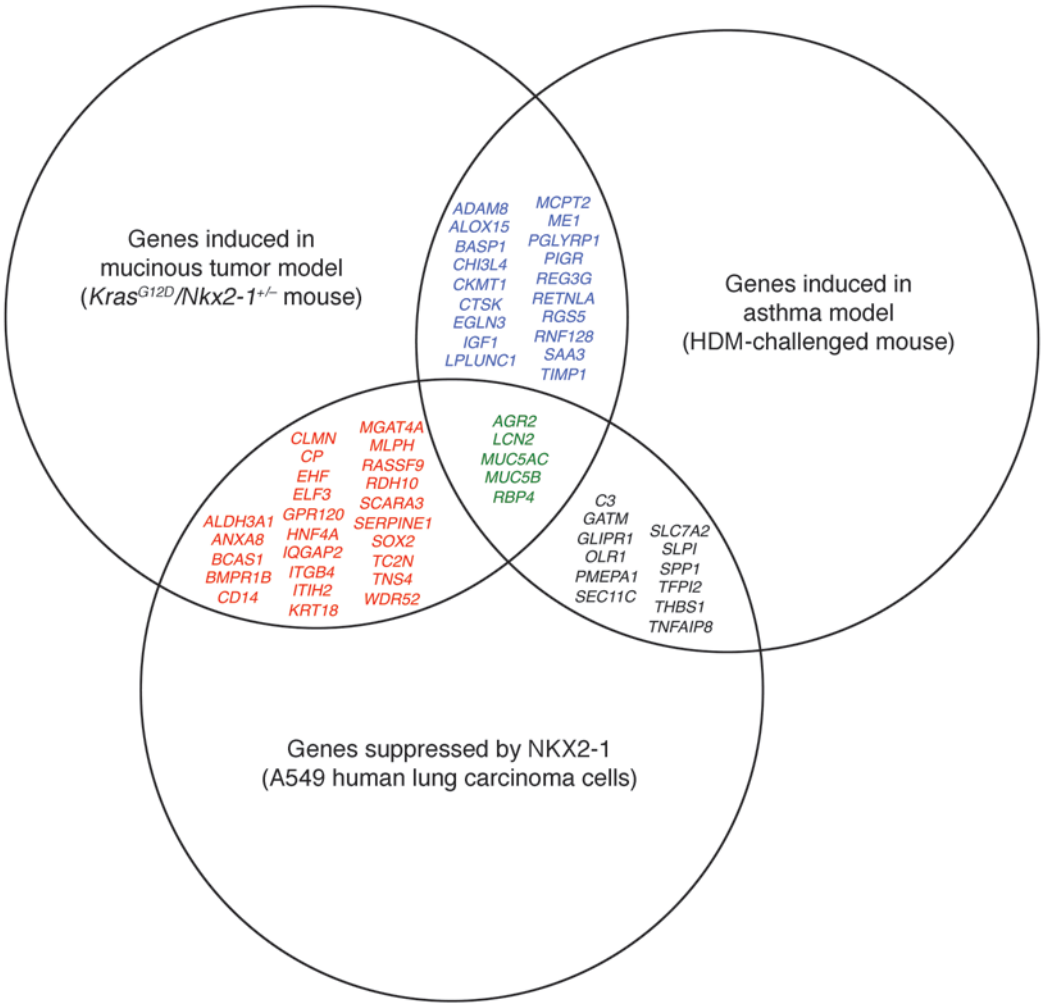

Figure 6
A subset of genes induced in the mucinous tumor model and the asthma model was suppressed by NKX2-1. Shown are results from 3 sets of mRNA microarray analysis (for simplicity, symbols for the human genes only are shown). For analysis of genes induced in mucinous tumors, mRNAs were isolated from lungs of control and *Kras*^{G12D}*;Nkx2-1*$^{+/-}$ mice and subjected to mRNA microarray analysis (n = 3 per group). For analysis of genes regulated by NKX2-1 in A549 human lung carcinoma cells, mRNAs were isolated from lentiviral *Nkx2-1*–expressing and control A549 cells and subjected to mRNA microarray analysis (n = 3 per group). For analysis of genes induced in asthma, mRNAs were isolated from lungs of control and HDM-challenged mice and subjected to mRNA microarray analysis (n = 3 per group) (23). Several mRNAs associated with mucous genes — *AGR2*, *MUC5AC*, and *MUC5B* — were induced in both the mucinous tumor and the asthma mouse models and suppressed by NKX2-1 in A549 human lung carcinoma cells. *HNF4A*, a non–lung lineage transcription factor, was suppressed by NKX2-1, a lung lineage transcription factor. *SOX2*, expressed in conducting airways but not in alveolar regions, was also suppressed by NKX2-1, and expressed in both conducting airways and alveoli.

inhibitory effect of NKX2-1 on *FGFR1* expression was blocked by PMA, an AP-1 inducer (Figure 8G). FOSL1 (a member of the AP-1 family; also known as FRA-1) induces colony formation of A549 cells (44). NKX2-1 inhibited FOSL1-mediated colony formation in A549 cells (Figure 8H). Thus, we concluded that NKX2-1 associates with AP-1 binding elements and inhibits both AP-1–mediated activity and tumor colony formation, providing a potential mechanism by which NKX2-1, at least in part, suppresses tumorigenesis.

Discussion

While the histology and prognosis of mucinous adenocarcinoma of the lung are well defined, experimental models for studying the pathogenesis and treatment of this cancer are lacking. In the present study, we created a mouse model of pulmonary mucinous adenocarcinoma by inducing mutant *Kras* in the respiratory epithelium of *Nkx2-1*$^{+/-}$ mice. Consistent with findings in human mucinous adenocarcinoma, these tumors contained numerous goblet cells that stained for mucins and expressed CK7 and CK20. Characteristics of the tumor-associated goblet cells were distinct from those in nontumorigenic intestine and airways. In contrast to findings in the *Kras*^{G12D}*;Nkx2-1*$^{+/-}$ mice, expression of mutant *EGFR* in the respiratory epithelium of *Nkx2-1*$^{+/-}$ mice did not cause mucinous tumors. Although KRAS and EGFR signaling pathways are shared, our findings indicate that the *Kras* mutation defines distinctive mucinous lung tumor pathology (Figure 9). Thus, our mouse model provides an experimental tool to under-

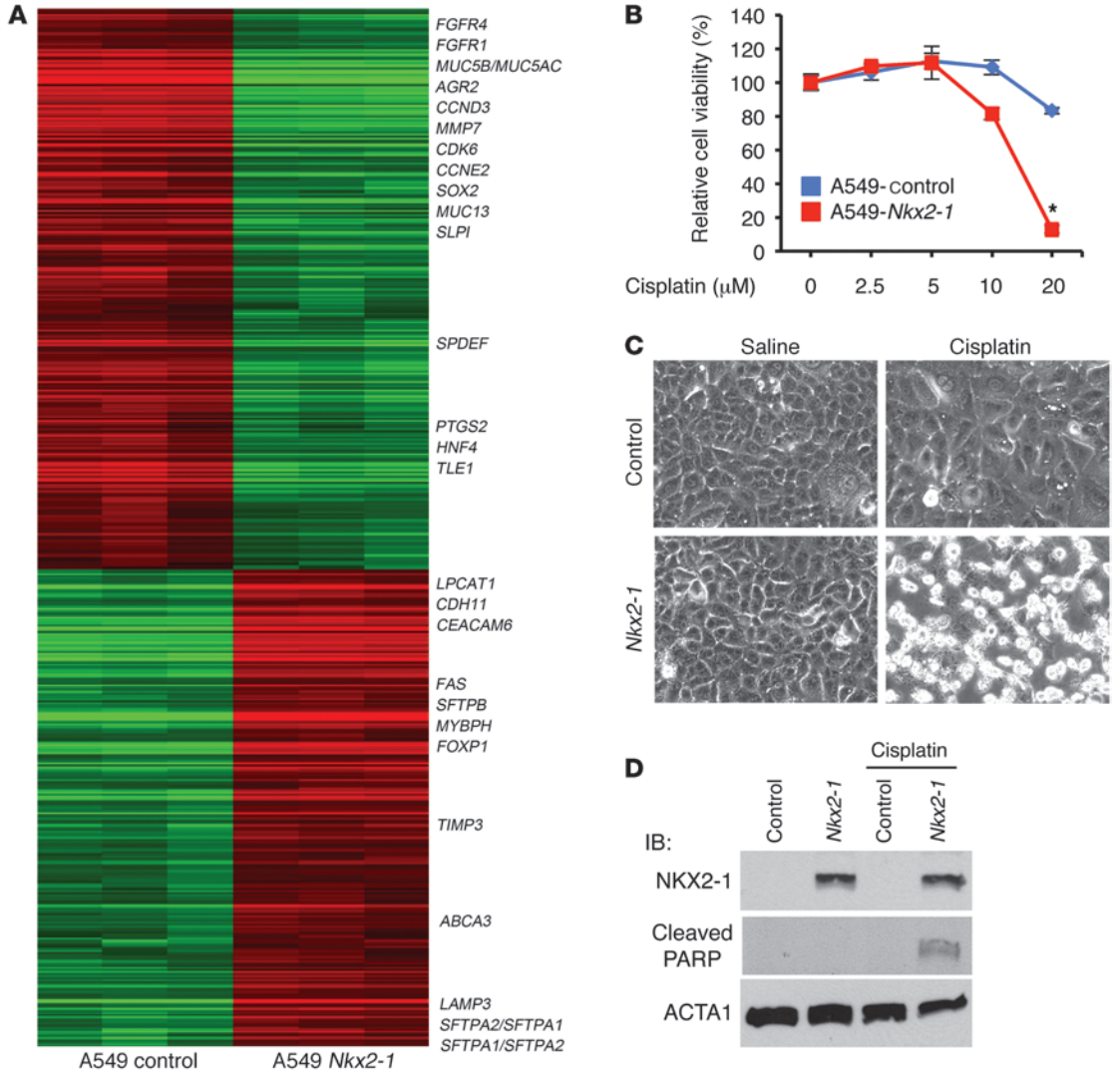

Figure 7

NKX2-1 inhibited mRNAs associated with tumorigenesis and induced those related to apoptosis. (**A**) mRNAs were isolated from lentiviral *Nkx2-1*–expressing and control A549 cells and subjected to mRNA microarray analysis. A heat map of the mRNAs is shown. Green and red denote mRNAs decreased and increased, respectively, by NKX2-1. mRNAs associated with mucus (*MUC5AC*, *MUC5B*, *MUC13*, and *AGR2*) and oncogenes (*FGFR1* and *CDK6*) were suppressed by NKX2-1. NKX2-1 induced surfactant protein genes (*SFTPA1* and *SFTPB*) and apoptotic genes (*FAS* and *TIMP3*). (**B**) Lentiviral *Nkx2-1*–expressing and control A549 cells were treated with cisplatin (final concentration, 0–20 μM). 72 hours after treatment, MTS assay was used to measure cell viability ($n = 3$ per group). Cisplatin treatment reduced *Nkx2-1*–expressing A549 carcinoma cell viability significantly more than that of control A549 cells. (**C**) Phase-contrast images of control and *Nkx2-1*–expressing A549 cells 24 hours after 20 μM cisplatin (original magnification, ×20). (**D**) NKX2-1 sensitized A549 cells to cisplatin-induced apoptosis. 24 hours after cisplatin treatment (20 μM), proteins were extracted from control or *Nkx2-1*–expressing A549 cells. Induction of cleaved PARP, an apoptosis marker, was confirmed by IB. Results are mean ± SD. *$P < 0.001$ vs. control.

stand the molecular mechanism causing pulmonary mucinous adenocarcinoma and may therefore be useful in identifying therapeutic targets for this disease.

Potential mechanisms of lung tumor goblet cell metaplasia/hyperplasia. The molecular mechanisms regulating airway goblet cell differentiation are being actively investigated. NKX2-1 and FOXA2 were downregulated in nontumorigenic airway goblet cells (15, 45), and transgenic expression of NKX2-1 or FOXA2 inhibited allergen-induced airway goblet cell metaplasia (4, 16). In the present study, both NKX2-1 and FOXA2 were inhibited in tumor goblet cells of $Kras^{G12D}$;$Nkx2\text{-}1^{+/-}$ mice, in which continuous (or chronic) reduction of *Nkx2-1* was achieved. This finding is consistent with their loss in goblet cells being associated with chronic lung diseases (4, 45). In contrast, SPDEF and FOXA3, which are normally induced during non–tumor-associated mucous metaplasia in the lung (15, 17), were not expressed in tumor goblet cells in $Kras^{G12D}$;$Nkx2\text{-}1^{+/-}$ mice, which indicates that mucin production in tumor goblet cells was not dependent on the SPDEF/FOXA3 transcriptional program. Likewise, this transcriptional program was not associated with goblet cell metaplasia in idiopathic pulmonary fibrosis (46).

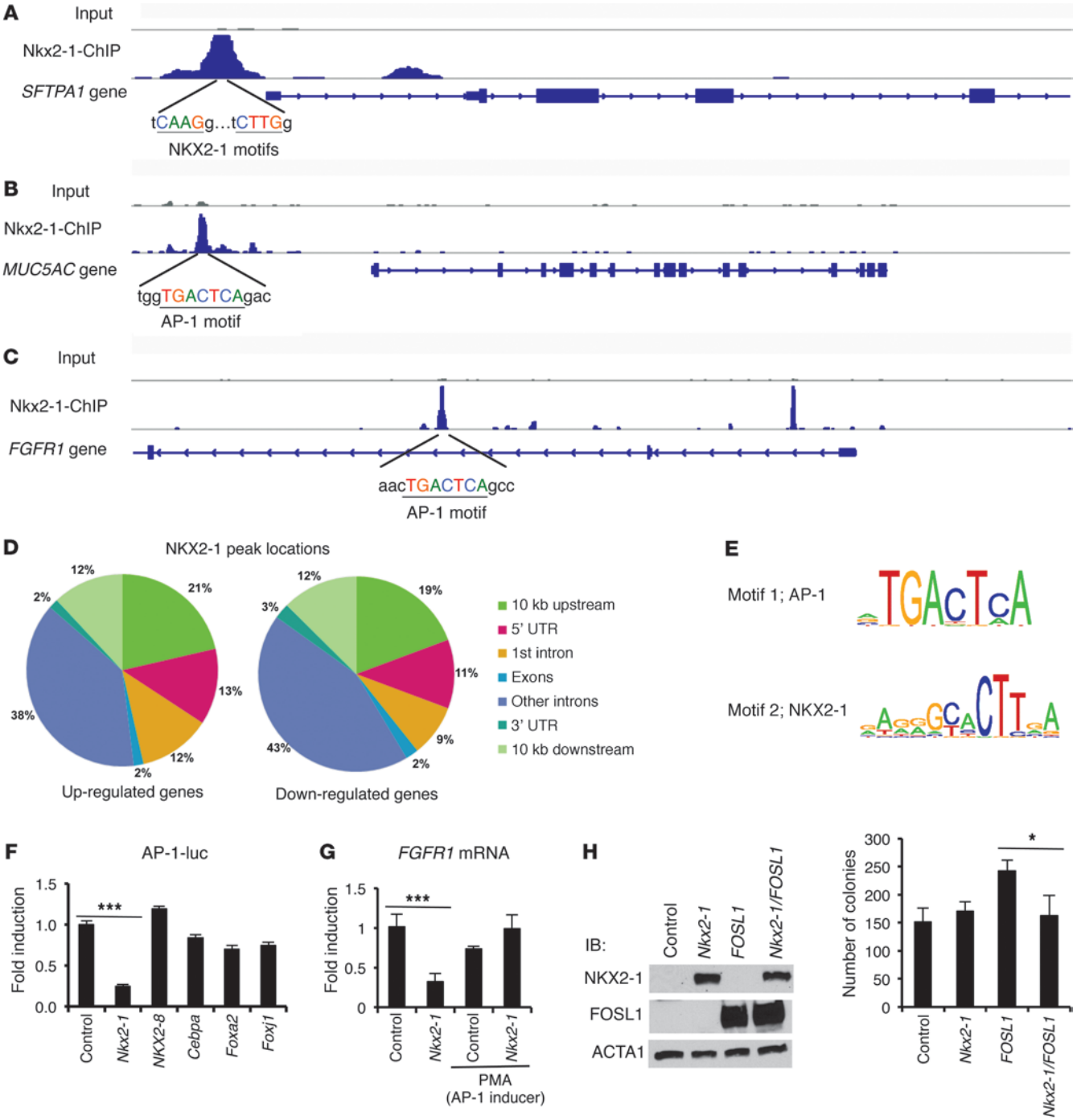

Figure 8

Identification of NKX2-1 binding sites by ChIP-seq. (**A**) NKX2-1 associated with the promoter and first intron of *SFTPA1* at sites that contain canonical NKX2-1 binding motifs (CAAG and CTTG). (**B**) NKX2-1 associated with the promoter of *MUC5AC* that contains an AP-1 binding motif (TGACTCA). (**C**) NKX2-1 associated with the first and second introns of *FGFR1*. (**D**) Distribution of peaks of NKX2-1 binding sites in genes up- or downregulated by NKX2-1. (**E**) Motifs present in NKX2-1 ChIP-seq peaks. (**F**) H441 lung adenocarcinoma cells were transfected as described in Methods. Results are presented as fold activation of light unit, normalized to β-galactosidase activity, relative to control constructs. NKX2-1 inhibited AP-1 activity in H441 cells (n = 3 per group). (**G**) Lentiviral *Nkx2-1*–expressing and control A549 cells were treated with PMA, an AP-1 inducer, at a final concentration of 10 ng/ml. *FGFR1* mRNA was measured as described in Methods. PMA rescued the inhibitory effect of NKX2-1 on *FGFR1* mRNA expression. (**H**) A549 cells stably expressing *Nkx2-1*, *FOSL1*, or both were developed using lentiviral vectors. Protein expression of NKX2-1 and FOSL1 was confirmed by IB. FOSL1-induced colony formation was inhibited by NKX2-1, as determined by soft agar assays (see Methods) performed using the stably infected cells and A549 control cells. n = 3 per group. Results are mean ± SD of biological triplicates for each group. *P < 0.05; **P < 0.01; ***P < 0.001.

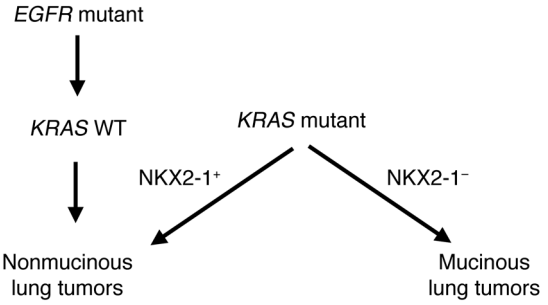

Figure 9
Inhibitory role of NKX2-1 in mucinous adenocarcinoma of the lung.

NKX2-1 functioned in a context-dependent manner to inhibit mutant KRAS tumorigenesis. The chromosomal region of 14q13.3 that is amplified in 10% of human lung adenocarcinoma (5–7) contains *MBIP*, *STELLAR.1*, *SFTA3*, *NKX2-1*, *NKX2-1-AS1*, *NKX2-8*, and *PAX9* (Ensembl genome browser; http://useast.ensembl.org/index.html). The role of this amplification in pulmonary oncogenesis has been of considerable interest. Loss-of-function and gain-of-function studies in vitro implicated *NKX2-1* as a potential oncogene (5–9). Recent studies using lung cancer mouse models did not support the proposed role of *NKX2-1* as a tissue-specific oncogene, but rather implicated NKX2-1 as an antimetastatic factor (10, 11). Furthermore, reduced expression of *Nkx2-1* induced cell proliferation and promoted carcinogen-induced thyroid adenoma in vivo (47). In the present study, NKX2-1 suppressed *Kras* tumorigenesis, but promoted *EGFR* tumorigenesis, in the transgenic mouse models. In $Kras^{LSL-G12D/+};p53^{-/-}$ mice, NKX2-1 functioned as an antimetastatic factor (10); however, in the present study, haploinsufficiency of *Nkx2-1* did not induce metastasis in either the $Kras^{G12D}$ or the $EGFR^{L858R}$ mouse model in vivo (data not shown). *Kras* mutation in combination with *p53*, $p16^{INK4a}$, or *Lkb1* deletion leads to lung tumor metastasis in mouse models (48). Since amplification of *NKX2-1* at the 14q13.3 locus is associated with a poor prognosis, whereas NKX2-1 protein levels are associated with a favorable prognosis (49), we assessed whether other genes located at the 14q13.3 locus might contribute to lung tumorigenesis in the mouse model. Expression of NKX2-1 with either NKX2.8 or PAX9 did not induce lung tumors in transgenic mice in vivo (Supplemental Figure 5). These results are consistent with prior reports that *Nkx2-8* null mice develop airway dysplasia at 1 year of age (50) and that expression of NKX2-8 inhibits growth of some lung cancer cells in vitro (51).

Identification of NKX2-1 downstream genes involved in mucinous tumorigenesis. The multiple genome-wide gene expression analyses combined with the NKX2-1 ChIP-seq analysis identified a set of NKX2-1–targeted genes involved in mucinous tumorigenesis. *RASSF9*, *SCARA3*, and *RDH10* were selectively induced in the mucinous tumor model, but not in the HDM-induced asthma model (Figure 6). These 3 genes were previously identified as NKX2-1 target genes in $Kras^{LSL-G12D/+};p53^{-/-}$ mice (10), which perhaps indicates that they are involved in tumor progression, but not goblet cell metaplasia/hyperplasia. Among the same set of genes, the lineage-specific transcription factors *HNF4A* and *SOX2* were also identified as genes suppressed by NKX2-1. NKX2-1 directly associated with the promoters of *HNF4A* and *SOX2* genes (Figure 6, Figure 7A, and Supplemental Figure 10). Tissue distribution of both HNF4A and SOX2 is distinct from that of NKX2-1. HNF4A, required for liver function, is expressed in the gastrointestinal system, liver, kidney, white adipose tissue, and pancreas, but not in normal lung, thyroid, or brain, where NKX2-1 is expressed (www.nursa.org/10.1621/datasets.02001). Both SOX2 and NKX2-1 are expressed in the respiratory tract. However, SOX2 is limited to conducting airway epithelial cells, whereas NKX2-1 is expressed in both conducting airways and the alveoli (52). NKX2-1 directly suppressed expression of *HNF4A* and *SOX2*, which in turn may influence tissue-specific cell specification. Regarding lung tumorigenesis, *SOX2* has been proposed as an oncogene in squamous cell lung carcinoma (53).

In summary, haploinsufficiency of *Nkx2-1* combined with $Kras^{G12D}$, but not $EGFR^{L858R}$, caused mucinous adenocarcinoma of the lung. The tumor goblet cells expressed a transcriptional program distinct from goblet cells induced by allergen exposure or those in intestine. NKX2-1 suppressed lung tumorigenesis caused by *Kras* mutation, but promoted lung tumorigenesis caused by *EGFR* mutation. ChIP-seq and mRNA microarray analysis revealed that NKX2-1 served distinct inhibitory and stimulatory roles in regulating the expression of genes involved in mucus production and lung tumorigenesis. Our results demonstrated the context-dependent role of NKX2-1 in the regulation of pulmonary adenocarcinoma, indicating that distinct approaches may be required for treatment of mucinous adenocarcinoma of the lung.

Methods

Human specimens. Pathologic tissues from mucinous (n = 6) and nonmucinous (n = 1) adenocarcinomas of the lung were obtained in accordance with institutional guidelines for use of human tissue for research purposes. See Supplemental Table 1 for patient information.

Transgenic mice and animal husbandry. $Nkx2\text{-}1^{+/-}$ mice were provided by S. Kimura (NIH, Bethesda, Maryland, USA; ref. 13). Transgenic mice bearing $[tetO]\text{-}EGFR^{L858R}$ (18) were obtained from the National Cancer Institute Mouse Repository. Transgenic mice bearing *Scgb1a1-rtTA*, $[tetO]\text{-}Kras4b^{G12D}$, and *[tetO]–Flag–Nkx2-1* were generated previously (4, 12). Transgenic mice bearing *[tetO]–NKX2-8* (human) and *[tetO]-PAX9* (human) were generated at the Transgenic and Gene Targeting Core at Cincinnati Children's Hospital Medical Center. Transgenic mice were provided chow containing Dox (625 mg/kg chow) beginning at 4–5 weeks of age. For urethane-induced tumorigenesis, control and *Nkx2-1* transgenic mice were injected i.p. with 1 mg/g body weight of urethane once weekly for 4 consecutive weeks after Dox administration. At 16 weeks after the first urethane injection, lungs were harvested, and tumors were counted using a dissecting microscope (20). See Supplemental Methods for animal maintenance.

MicroCT imaging and tumor count and volume measurement. See Supplemental Methods.

Tissue preparation, immunohistochemistry, and immunofluorescence microscopy. Staining (H&E, Alcian blue, and immunohistochemistry) was performed using 5-μm paraffin-embedded lung sections as previously described (15). See Supplemental Methods for antibody information.

Cell lines. See Supplemental Methods.

mRNA microarray and expression analyses. RNA isolation and microarray analysis were performed as previously described (4). Differentially expressed genes were identified using a random-variance t test (54). Gene identifications were considered statistically significant if their P value was less than 0.01, false discovery rate was less than 5%, and fold change was greater than 2.0. Microarray results were deposited in GEO (accession nos. GSE40508 and GSE40584). See Supplemental Methods for Gene Ontology analysis and quantitative RT-PCR.

Immunoblot assays. See Supplemental Methods.

Transient transfection assays. See Supplemental Methods.

Treatment of A549 cells with cisplatin or PMA. See Supplemental Methods.

ChIP-seq analysis. ChIP was performed using rabbit anti–NKX2-1 antibody (catalog no. WRAB-1231; Seven Hills Bioreagents) with chromatin from NKX2-1–expressing A549 lung carcinoma cells according to the manufacturer's protocol (catalog no. 9003; Cell Signaling Technology). ChIP-enriched DNA (10 ng) or input DNA was used for high-throughput DNA sequencing. The samples were blunt ended, A-tailed, and ligated with adaptors, according to the library preparation protocol from Illumina. DNA fragments approximately 250 bp in length were size-selected and amplified. ChIP-enriched and input DNA samples were barcoded and sequenced simultaneously for 50 cycles using Solexa/Illumina Genome Analyzer II at the University of California, Riverside. Sequenced reads (6 bp linker plus 45 bp DNA) were demultiplexed based on the 6-bp barcodes, and barcodes were removed before alignment. Alignment of sequence reads to the human reference (assembly hg19) was performed using Bowtie (55). ChIP-seq read density files were generated and viewed in the Integrative Genome Viewer (IGV; ref. 56). To determine where NKX2-1 bound to the genome, enrichment peaks were detected and subsequently mapped to the nearest annotated genes using CisGenome software (57). See Supplemental Methods for motif frequency analysis. Consensus motifs (Figure 8E and Supplemental Figure 9C) were computed using Gibbs Motif Sampler provided by CisGenome using the default parameters.

Soft agar colony formation assays. See Supplemental Methods.

Statistics. Statistical differences were determined using Student's *t* test (2-tailed and unpaired) or Mann-Whitney test. The difference between 2 groups was considered significant when the *P* value was less than 0.05 for all tests of mouse and in vitro experiments.

Study approval. The animal protocol was reviewed and approved by the Institutional Animal Care and Use Committee at the Cincinnati Children's Hospital Medical Center. Human specimen analysis was approved by the ethics committees of Nagasaki Graduate School of Biomedical Sciences (permission no. 05062433-2) and Kawasaki Medical School (permission no. 255), and written informed consent was obtained from all participants before study entry.

Acknowledgments

This study was supported by NIH grants to J.A. Whitsett (HL110964, HL095580, and HL108907) and Y. Xu (HL105433); by the Ministry of Education, Science, and Culture of Japan to T. Tsuchiya, T. Fukazawa, Y. Naomoto, and T. Nagayasu; and by the University of Cincinnati Postdoctoral Fellow Research Program to Y. Maeda. The authors thank I. Fink-Baldauf, R. Pratt, I-C. Wang, G. Chen, S. Smith, L. Zhang, S. Wert, S. Kimura, and J. Minna for materials and technical assistance and K. Wikenheiser-Brokamp, H. Miyoshi, T. Suzuki, M. Durbin, and F. Sladek for discussions.

Received for publication March 27, 2012, and accepted in revised form September 6, 2012.

Address correspondence to: Jeffrey A. Whitsett, Cincinnati Children's Hospital Medical Center, Section of Neonatology, Perinatal and Pulmonary Biology, 3333 Burnet Avenue, MLC7029, Cincinnati, Ohio 45229-3039, USA. Phone: 513.803.2790; Fax: 513.636.7868; E-mail: jeff.whitsett@cchmc.org.

1. Travis WD, et al. International association for the study of lung cancer/american thoracic society/european respiratory society international multidisciplinary classification of lung adenocarcinoma. *J Thorac Oncol*. 2011;6(2):244–285.
2. Subramanian J, Govindan R. Molecular genetics of lung cancer in people who have never smoked. *Lancet Oncol*. 2008;9(7):676–682.
3. Maeda Y, Davé V, Whitsett JA. Transcriptional control of lung morphogenesis. *Physiol Rev*. 2007;87(1):219–244.
4. Maeda Y, et al. Airway epithelial transcription factor NK2 homeobox 1 inhibits mucous cell metaplasia and Th2 inflammation. *Am J Respir Crit Care Med*. 2011;184(4):421–429.
5. Kendall J, et al. Oncogenic cooperation and coamplification of developmental transcription factor genes in lung cancer. *Proc Natl Acad Sci U S A*. 2007;104(42):16663–16668.
6. Weir BA, et al. Characterizing the cancer genome in lung adenocarcinoma. *Nature*. 2007; 450(7171):893–898.
7. Kwei KA, et al. Genomic profiling identifies TITF1 as a lineage-specific oncogene amplified in lung cancer. *Oncogene*. 2008;27(25):3635–3640.
8. Tanaka H, et al. Lineage-specific dependency of lung adenocarcinomas on the lung development regulator TTF-1. *Cancer Res*. 2007;67(13):6007–6011.
9. Yamaguchi T, et al. NKX2-1/TITF1/TTF-1-induced ROR1 is required to sustain EGFR survival signaling in lung adenocarcinoma. *Cancer Cell*. 2012;21(3):348–361.
10. Winslow MM, et al. Suppression of lung adenocarcinoma progression by Nkx2-1. *Nature*. 2011;473(7345):101–104.
11. Hosono Y, et al. MYBPH, a transcriptional target of TTF-1, inhibits ROCK1, and reduces cell motility and metastasis. *EMBO J*. 2011;31(2):481–493.
12. Fisher GH, et al. Induction and apoptotic regression of lung adenocarcinomas by regulation of a K-Ras transgene in the presence and absence of tumor suppressor genes. *Genes Dev*. 2001;15(24):3249–3262.
13. Kimura S, et al. The T/ebp null mouse: thyroid-specific enhancer-binding protein is essential for the organogenesis of the thyroid, lung, ventral forebrain, and pituitary. *Genes Dev*. 1996;10(1):60–69.
14. Zhang Y, et al. GATA and Nkx factors synergistically regulate tissue-specific gene expression and development in vivo. *Development*. 2007;134(1):189–198.
15. Chen G, et al. SPDEF is required for mouse pulmonary goblet cell differentiation and regulates a network of genes associated with mucus production. *J Clin Invest*. 2009;119(10):2914–2924.
16. Chen G, et al. Foxa2 programs Th2 cell-mediated innate immunity in the developing lung. *J Immunol*. 2010;184(11):6133–6141.
17. Park KS, et al. SPDEF regulates goblet cell hyperplasia in the airway epithelium. *J Clin Invest*. 2007;117(4):978–988.
18. Politi K, Zakowski MF, Fan PD, Schonfeld EA, Pao W, Varmus HE. Lung adenocarcinomas induced in mice by mutant EGF receptors found in human lung cancers respond to a tyrosine kinase inhibitor or to down-regulation of the receptors. *Genes Dev*. 2006;20(11):1496–1510.
19. Engelman JA, et al. Effective use of PI3K and MEK inhibitors to treat mutant Kras G12D and PIK3CA H1047R murine lung cancers. *Nat Med*. 2008;14(12):1351–1356.
20. Stathopoulos GT, et al. Epithelial NF-kappaB activation promotes urethane-induced lung carcinogenesis. *Proc Natl Acad Sci U S A*. 2007; 104(47):18514–18519.
21. Malkinson AM. Primary lung tumors in mice as an aid for understanding, preventing, and treating human adenocarcinoma of the lung. *Lung Cancer*. 2001;32(3):265–279.
22. Ramirez RD, et al. Immortalization of human bronchial epithelial cells in the absence of viral oncoproteins. *Cancer Res*. 2004;64(24):9027–9034.
23. Lewis CC, et al. Unique and overlapping gene expression patterns driven by IL-4 and IL-13 in the mouse lung. *J Allergy Clin Immunol*. 2009; 123(4):795–804.
24. Kolla V, et al. Thyroid transcription factor in differentiating type II cells: regulation, isoforms, and target genes. *Am J Respir Cell Mol Biol*. 2007;36(2):213–225.
25. Saito RA, et al. Thyroid transcription factor-1 inhibits transforming growth factor-beta-mediated epithelial-to-mesenchymal transition in lung adenocarcinoma cells. *Cancer Res*. 2009;69(7):2783–2791.
26. Behrens C, et al. Immunohistochemical expression of basic fibroblast growth factor and fibroblast growth factor receptors 1 and 2 in the pathogenesis of lung cancer. *Clin Cancer Res*. 2008;14(19):6014–6022.
27. Spinola M, et al. Functional FGFR4 Gly388Arg polymorphism predicts prognosis in lung adenocarcinoma patients. *J Clin Oncol*. 2005; 23(29):7307–7311.
28. Fürstenberger G, Senn HJ. Insulin-like growth factors and cancer. *Lancet Oncol*. 2002;3(5):298–302.
29. Chen BB, Glasser JR, Coon TA, Mallampalli RK. F-box protein FBXL2 exerts human lung tumor suppressor-like activity by ubiquitin-mediated degradation of cyclin D3 resulting in cell cycle arrest. *Oncogene*. 2012;31(20):2566–2579.
30. Wang IC, Meliton L, Tretiakova M, Costa RH, Kalinichenko VV, Kalin TV. Transgenic expression of the forkhead box M1 transcription factor induces formation of lung tumors. *Oncogene*. 2008;27(30):4137–4149.
31. Laman H, et al. Transforming activity of Fbxo7 is mediated specifically through regulation of cyclin D/cdk6. *EMBO J*. 2005;24(17):3104–3116.
32. Owen-Schaub LB. Fas function and tumor progression: use it and lose it. *Cancer Cell*. 2002;2(2):95–96.
33. Finan KM, et al. In vitro susceptibility to the proapoptotic effects of TIMP-3 gene delivery translates to greater in vivo efficacy versus gene delivery for TIMPs-1 or -2. *Lung Cancer*. 2006;53(3):273–284.
34. Anagnostou VK, Syrigos KN, Bepler G, Homer RJ, Rimm DL. Thyroid transcription factor 1 is

an independent prognostic factor for patients with stage I lung adenocarcinoma. *J Clin Oncol*. 2009;27(2):271–278.
35. O'Byrne KJ, et al. Molecular biomarkers in non-small-cell lung cancer: a retrospective analysis of data from the phase 3 FLEX study. *Lancet Oncol*. 2011;12(8):795–805.
36. Bruno MD, Bohinski RJ, Huelsman KM, Whitsett JA, Korfhagen TR. Lung cell-specific expression of the murine surfactant protein A (SP-A) gene is mediated by interactions between the SP-A promoter and thyroid transcription factor-1. *J Biol Chem*. 1995;270(12):6531–6536.
37. Islam KN, Mendelson CR. Permissive effects of oxygen on cyclic AMP and interleukin-1 stimulation of surfactant protein A gene expression are mediated by epigenetic mechanisms. *Mol Cell Biol*. 2006;26(8):2901–2912.
38. MacQuarrie KL, Fong AP, Morse RH, Tapscott SJ. Genome-wide transcription factor binding: beyond direct target regulation. *Trends Genet*. 2011;27(4):141–148.
39. Majewski J, Ott J. Distribution and characterization of regulatory elements in the human genome. *Genome Res*. 2002;12(12):1827–1836.
40. Bohinski RJ, Di Lauro R, Whitsett JA. The lung-specific surfactant protein B gene promoter is a target for thyroid transcription factor 1 and hepatocyte nuclear factor 3, indicating common factors for organ-specific gene expression along the foregut axis. *Mol Cell Biol*. 1994;14(9):5671–5681.
41. Heintz NH, Janssen-Heininger YM, Mossman BT. Asbestos, lung cancers, and mesotheliomas: from molecular approaches to targeting tumor survival pathways. *Am J Respir Cell Mol Biol*. 2010;42(2):133–139.
42. Gensch E, et al. Tobacco smoke control of mucin production in lung cells requires oxygen radicals AP-1 and JNK. *J Biol Chem*. 2004; 279(37):39085–39093.
43. Kato S, et al. MUC5AC mucin gene regulation in pancreatic cancer cells. *Int J Oncol*. 2006;29(1):33–40.
44. Adiseshaiah P, Lindner DJ, Kalvakolanu DV, Reddy SP. FRA-1 proto-oncogene induces lung epithelial cell invasion and anchorage-independent growth in vitro, but is insufficient to promote tumor growth in vivo. *Cancer Res*. 2007;67(13):6204–6211.
45. Wan H, et al. Foxa2 regulates alveolarization and goblet cell hyperplasia. *Development*. 2004; 131(4):953–964.
46. Plantier L, et al. Ectopic respiratory epithelial cell differentiation in bronchiolised distal airspaces in idiopathic pulmonary fibrosis. *Thorax*. 2011;66(8):651–657.
47. Hoshi S, et al. Role of NKX2-1 in N-bis(2-hydroxypropyl)-nitrosamine-induced thyroid adenoma in mice. *Carcinogenesis*. 2009;30(9):1614–1619.
48. Ji H, et al. LKB1 modulates lung cancer differentiation and metastasis. *Nature*. 2007;448(7155):807–810.
49. Tang X, et al. Abnormalities of the TITF-1 lineage-specific oncogene in NSCLC: implications in lung cancer pathogenesis and prognosis. *Clin Cancer Res*. 2011;17(8):2434–2443.
50. Tian J, Mahmood R, Hnasko R, Locker J. Loss of Nkx2.8 deregulates progenitor cells in the large airways and leads to dysplasia. *Cancer Res*. 2006;66(21):10399–10407.
51. Harris T, et al. Both gene amplification and allelic loss occur at 14q13.3 in lung cancer. *Clin Cancer Res*. 2011;17(4):690–699.
52. Whitsett JA, Haitchi HM, Maeda Y. Intersections between pulmonary development and disease. *Am J Respir Crit Care Med*. 2011;184(4):401–406.
53. Bass AJ, et al. SOX2 is an amplified lineage-survival oncogene in lung and esophageal squamous cell carcinomas. *Nat Genet*. 2009;41(11):1238–1242.
54. Wright GW, Simon RM. A random variance model for detection of differential gene expression in small microarray experiments. *Bioinformatics*. 2003;19(18):2448–2455.
55. Langmead B, Trapnell C, Pop M, Salzberg SL. Ultrafast and memory-efficient alignment of short DNA sequences to the human genome. *Genome Biol*. 2009;10(3):R25.
56. Robinson JT, et al. Integrative genomics viewer. *Nat Biotechnol*. 2011;29(1):24–26.
57. Ji H, Jiang H, Ma W, Johnson DS, Myers RM, Wong WH. An integrated software system for analyzing ChIP-chip and ChIP-seq data. *Nat Biotechnol*. 2008;26(11):1293–1300.